Available online at www.sciencedirect.com

ScienceDirect

Virology 367 (2007) 348–357

VIROLOGY

www.elsevier.com/locate/yviro

Membrane insertion and topology of the p7B movement protein of *Melon Necrotic Spot Virus* (MNSV)

Luis Martínez-Gil [a], Ana Saurí [a], Marçal Vilar [a], Vicente Pallás [b], Ismael Mingarro [a,*]

[a] *Departament de Bioquímica i Biologia Molecular, Universitat de València. E-46 100 Burjassot, Spain*

[b] *Instituto de Biología Molecular y Celular de Plantas, Universidad Politécnica de Valencia-CSIC, Avenida de los Naranjos s/n, E-46022 Valencia, Spain*

Received 13 March 2007; returned to author for revision 31 May 2007; accepted 6 June 2007

Available online 3 July 2007

Abstract

Cell-to-cell movement of the *Melon Necrotic Spot Virus* (MNSV) is controlled by two small proteins working *in trans*, an RNA-binding protein (p7A) and an integral membrane protein (p7B) separated by an amber stop codon. p7B contains a single hydrophobic region. Membrane integration of this region was observed when inserted into model proteins in the presence of microsomal membranes. Furthermore, we explored the topology and targeting mechanisms of full-length p7B. Here we present evidence that p7B integrates in vitro into the ER membrane cotranslationally and with an Nt-cytoplasmic/Ct-luminal orientation. The observed topology was monitored in vivo by fusing GFP to the Ct of p7B, enabling the overexpression in *Escherichia coli* cultures. Finally, the topology of a putative p14 movement protein was established by replacing the amber stop codon located between p7A and p7B.

Keywords: MNSV; Movement proteins; Plant virus; Membrane integration; Membrane protein topology

Introduction

Plant viruses move from the initially infected cell to neighboring cells and then throughout the host in an active process that requires the function of virus-coded movement proteins (MPs). MPs are specialized proteins that are essential for the translocation of viral genomes or virions from the replication sites to plasmodesmata and then to adjacent neighboring cells (Heinlein and Epel, 2004). In numerous cases, virus replication complexes (VRCs) are associated with biological membranes that include endoplasmic reticulum (ER), tonoplast, mitochondrial membranes, etc. (Lazarowitz and Beachy, 1999). It has been well documented that at least some of these VRCs also contain MPs (Mas and Beachy, 1999), in addition to viral RNA, viral replicase and several unidentified host proteins. The localization of MPs with cortical ER strongly suggests that virus replication, virus protein synthesis and intra- and inter-cellular movement are functionally linked processes. Plasmodesmata are the structures that mediate cell-to-cell communication in plants providing cytoplasmic and ER continuity (Lazarowitz and Beachy, 1999; Staehelin, 1997). Plant viral genomes display a range of complexity in terms of the number and type of viral proteins required for movement (Lucas, 2006). MP activities are best described in the tobacco mosaic tobamovirus (TMV) model system. TMV MP is a single multidomain protein that names the '30K' superfamily of MPs (Citovsky and Zambryski, 1991). The 30K TMV MP is able to bind viral RNA (Citovsky et al., 1992), to associate with ER membranes (Mas and Beachy, 1999) and the domains responsible for this association have been circumscribed (Fujiki et al., 2006).

Many virus genera possess not one, but two or three MPs. The genus *Carmovirus* has a transport system based on two small MPs. Sequence analysis of the *Turnip crinkle virus* (TCV) and the *Carnation mottled virus* (CarMV), the most thoroughly studied viruses of the *Carmovirus* genus, revealed that the two open reading frames (ORFs) involved in the movement process are overlapping. *Melon necrotic spot virus* (MNSV), a member

Abbreviations: Ct, C-terminus; ER, endoplasmic reticulum; Lep, leader peptidase; MMs, microsomal membranes; MNSV, melon necrotic spot virus; MP, movement protein; Nt, N-terminus; SDS-PAGE, sodium dodecylsulfate polyacryamide-gel electrophoresis; TM, transmembrane.

* Corresponding author. Fax: +34 96 354 4635.

E-mail address: Ismael.Mingarro@uv.es (I. Mingarro).

0042-6822/$ - see front matter © 2007 Elsevier Inc. All rights reserved.
doi:10.1016/j.virol.2007.06.006

of the genus *Carmovirus*, is a small isometric plant virus with a single-stranded, positive-sense RNA genome that encodes for at least five different proteins (Genoves et al., 2006; Riviere and Rochon, 1990). Several MNSV isolates have been cloned and sequenced (Diaz et al., 2003; Genoves et al., 2006). In contrast to that observed in the TCV and CarMV sequences, the genome organization of the MNSV is somehow unique since the centrally located ORFs that encode the two 7-kDa MPs (p7A and p7B proteins) are not overlapping but consecutive. In fact, both ORFs that have been revealed to be sufficient to support viral movement between adjacent cells operating in trans (Genoves et al., 2006), are separated by an amber stop codon. Interestingly, if translational read-through of the amber codon located at the end of p7A occurred, both proteins would be joined in frame, resulting in a fusion protein of 14 kDa (p14). Nevertheless, it is established that two sub-genomic RNAs (sgRNA) of approximately 1.9 kb and 1.6 kb, co-terminal with the 3′ genomic end, are produced during the MNSV infection cycle. The smaller sgRNA directs the translation of the coat protein while the larger one appears to be a bi-cistronic RNA that would direct the translation of the two central small proteins, p7A and p7B, through an uncharacterized mechanism (Riviere and Rochon, 1990; Russo et al., 1994).

Coordination between two small movement proteins (double gene block) has been previously postulated for the homologous MPs of *Carnation mottle virus* (CarMV) p7 and p9. Hence, an RNA-binding capacity for CarMV p7 has been demonstrated (Marcos et al., 1999; Vilar et al., 2001, 2005), as have the ER membrane targeting and cotranslational integration of CarMV p9 (Sauri et al., 2005, 2007; Vilar et al., 2002). Following the same pattern, in the case of MNSV we have recently shown that the viral genome binding function seems to be accomplished by p7A, whereas p7B could be involved in the association with the intracellular membrane system (Navarro et al., 2006), mapping both MP functions in the two separate polypeptides.

The current study provides additional information on the association of p7B with biological membranes. We have identified a single membrane-spanning domain in p7B by using an in vitro translation system of model integral membrane protein constructs in the presence of microsomal membranes (MMs). In addition, the membrane targeting and topology of the protein has been investigated in vitro. Furthermore, by fusing GFP to the C-terminus (Ct) of p7B we have monitored the membrane orientation of overexpressed fusion proteins in intact *Escherichia coli* cells. From these results, a preferential Nt-cytoplasmic/Ct-luminal topology for the MNSV p7B protein was deduced both in vitro and in vivo. Finally, we provide further data suggesting the same topology for the hypothetical p14 MP that could arise in the case of translation read-through of the amber stop codon located between the p7A and p7B proteins.

Results

Sequence analysis of the p7B movement protein

Amino acid sequence comparisons of p7B from MNSV and other homologue MPs from the genus *Carmovirus* showed one hydrophobic region (Navarro et al., 2006), suggesting the presence of only one transmembrane (TM) domain. As a useful starting point, we have used a number of programs available on the Internet to predict the topology of the p7B MP. It has been established that the reliability of a given predicted topology is very high when many different methods agree (Drew et al., 2002; Melen et al., 2003; Nilsson et al., 2000). We have submitted the p7B sequence to the most current web-versions of five popular prediction methods: TMHMM (Krogh et al., 2001), HMMTOP (Tusnady and Simon, 1998, 2001), MEMSAT (Jones, 2007; Jones et al., 1994), PHD (Rost et al., 1996) and TOPPRED (Claros and von Heijne, 1994; von Heijne, 1992). By way of example, Fig. 1b shows the probability of each residue being part of a TM segment using the TMHMM 2.0 software, a method that uses a hidden Markov model to predict TM helices in protein sequences (Krogh et al., 2001). The putative TM segment extends from tyrosine 13 to leucine 32 (Fig. 1a). The polar C-terminal domain is predicted to form a water-soluble region. The TMHMM server, as well as the rest of the algorithms used (not shown), also predicts the topology of the MNSV p7B protein, rendering its Nt inside the cell and its Ct outside (Fig. 1b).

Insertion of the MNSV p7B putative TM region into biological membranes

The membrane insertion of the p7B hydrophobic region was investigated by using an in vitro experimental system that accurately reports the integration of TM helices into MMs (Hessa et al., 2005a). Briefly, a segment to be tested (H-segment, Fig. 2) is engineered into the luminal P2 domain of the integral membrane protein leader peptidase (Lep) from *E. coli*, where it is flanked by two acceptor sites (G1 and G2) for N-linked glycosylation (Fig. 2a). This experimental system, based on the in vitro translation of engineered Lep in the presence of canine pancreatic microsomes, enables the measurement of the efficiency with which natural or designed polypeptide segments insert into the ER membrane under conditions approximating the in vivo situation (Hessa et al., 2005a,b; Sääf et al., 1998). Both engineered glycosylation sites will be used as a membrane insertion reporter. The rationale behind using two glycosylation sites is the following: G1 will always be glycosylated, due to its native luminal localization; instead, G2 will be glycosylated only upon translocation of the tested H-segment through the microsomal membrane. Thus, single glycosylation indicates a correct TM integration (Fig. 2a, left), whereas double glycosylation reports the non-integration capability of the tested H-segment (Fig. 2a, right). Single glycosylation of the molecule results in an increase in molecular mass of about 2.5 kDa relative to the observed molecular mass of Lep expressed in the absence of microsomes, and of around 5 kDa in the case of double glycosylation. The translation of the chimeric constructs harboring the predicted p7B TM region as H-segment mainly resulted in single glycosylated forms (Fig. 2b, lane 3), suggesting membrane integration of this region. Control constructs with computer-designed previously tested (Sääf

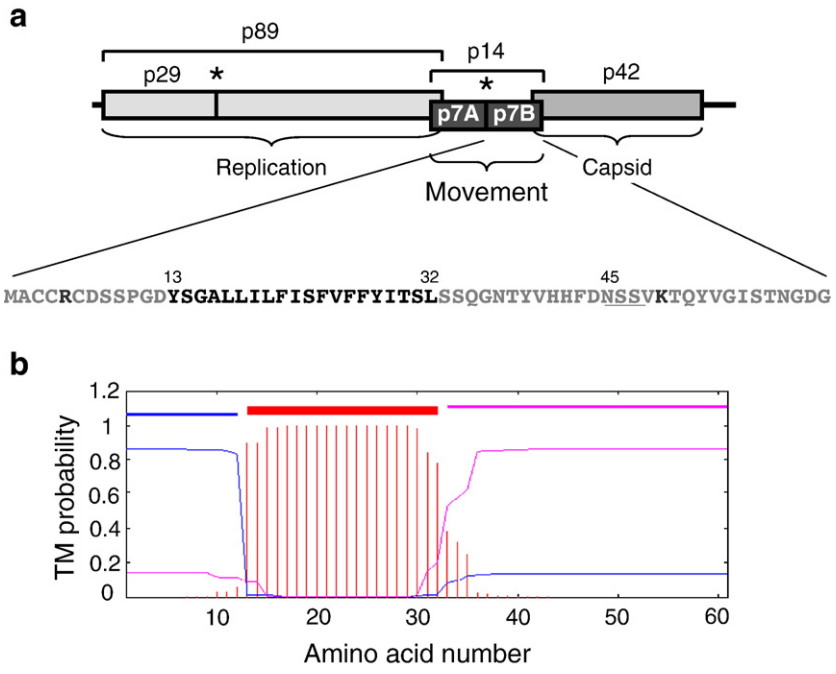

Fig. 1. (a) Diagrammatic representation of the MNSV ORFs highlighting the deduced amino acid sequence of the Spanish MNSV-A1 isolate (Genoves et al., 2006) (GenBank accession number DQ339157). Asterisks denote the position of amber stop codons. Amino acid residues of the hydrophobic region of p7B are shown in black and the positively charged residues in dark grey. A natural glycosylation site is underlined. (b) Topology prediction for the 61 amino acids of p7B using the TMHMM prediction method. p7B is predicted to have a single TM helix (13–32) with the Nt facing the cytoplasm and the C-terminal extramembranous domain located outside the cell. The TM domain (red rectangle), the cytoplasmic loop (blue line) and the luminal loop (pink line) are indicated above the curves that show the a posteriori probabilities for the different locations.

et al., 1998) non-integration and integration sequences are shown (Fig. 2b, lanes 1 and 2 respectively).

p7B integrates cotranslationally into the ER membrane through its single TM domain and with an Nt cytoplasmic/Ct luminal orientation

We have previously shown that the CarMV double-spanning p9 MP integrates into the ER membrane cotranslationally through the Sec61 translocon (Sauri et al., 2005, 2007). Since the integration of proteins into ER-derived microsomes can be monitored by glycosylation (Johnson and van Waes, 1999), we decided to investigate whether MNSV p7B is cotranslationally integrated into the ER membrane by using cycloheximide to block protein synthesis following the in vitro translation reaction. It is important to note that a possible N-linked glycosylation site is located downstream of the TM domain in the wild-type sequence (Fig. 1a), but not at a very efficient distance for proper glycosylation as it is only 13 residues away from the predicted TM segment. The minimum distance from the luminal end of a TM segment required for glycosylation when the acceptor site is downstream of the TM segment must be $\geq$12–13 residues (Nilsson and von Heijne, 1993). Since the Asn acceptor site in p7B is approximately positioned at this threshold (residue 45, with the predicted TM segment ending at residue 32, see Fig. 1a), low levels of glycosylation are expected in the p7B wild-type protein. Nevertheless, when full-length p7B was translated in vitro in the presence of microsomes the protein was significantly glycosylated (Fig. 3a, lanes 1 and 4), as shown by the increase in the electrophoretic mobility of the slower radioactive band after an endoglycosidase H (endo H) treatment (Fig. 3a, lane 6). However, when microsomes were absent or added post-translationally after the inhibition of protein synthesis with cycloheximide, no p7B was glycosylated (Fig. 3a, lanes 2, 3 and 5), thereby demonstrating that p7B movement protein cannot integrate post-translationally through the ER translocon. In addition, these experiments pointed towards a C-terminal luminal orientation of the p7B movement protein based on the glycosylation of the Ct portion.

In order to prove that p7B membrane integration relies on its single TM domain, a construct was engineered where the natural p7B glycosylation site was erased and the first 50 residues of the luminal P2 domain from Lep, containing a glycosylation site, were fused at the Ct of the movement protein (p7B/P2). Deletion of the hydrophobic region (residues 13–32) rendered p7BΔTM/P2 construct. In vitro transcription/translation experiments of these constructs were performed in the presence of ER-derived MMs. After centrifugation of the translation reaction mixture, proteins were recovered from a 100,000×*g* pelleted (membrane) fraction only when the TM domain was present (Fig. 3b), indicating that membrane association relies on the hydrophobic region. As above, glycosylation was observed by the appearance of a larger protein band in the pellet fraction of the p7B/P2 construct (Fig. 3b, lane 2), suggesting a preferential C-terminal luminal orientation of the chimera. Nonetheless, the co-existence of molecules with the reversed topology cannot be

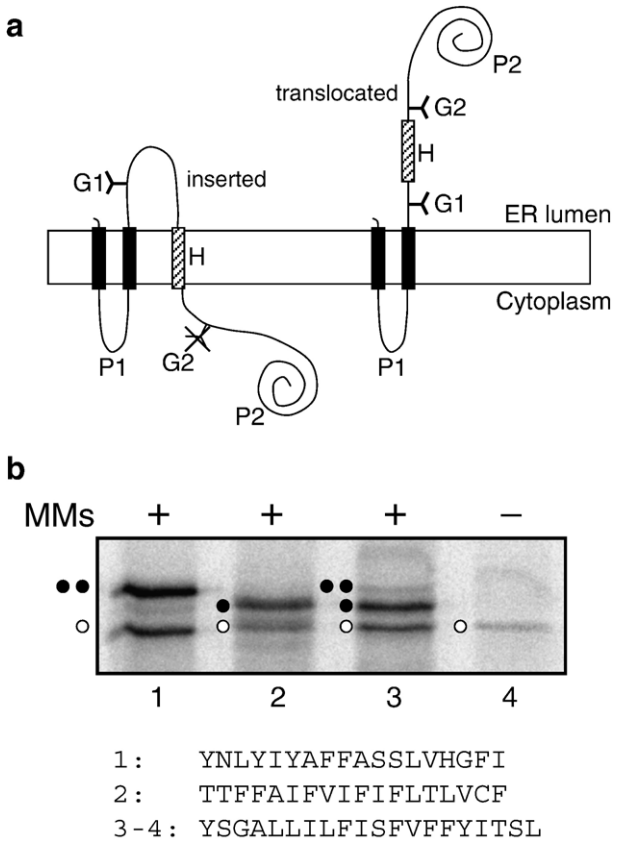

Fig. 2. The engineered leader peptidase (Lep) model protein. (a) Wild-type Lep has two TM helices (H1, H2) and a large C-terminal lumenal domain (P2). It inserts into microsomal membranes (MMs) in an Nt/Ct luminal orientation. H-segments were inserted in the P2 domain flanked by two glycosylation acceptor sites (G1 and G2) (Hessa et al., 2005a). For the H-segments that integrate into the membrane, only the G1 site is glycosylated (left), whereas both the G1 and G2 sites are glycosylated for the H-segments that do not integrate into the membrane (right). (b) In vitro translation in the presence (+) of MMs. Control H-segments were used to verify sequence translocation (lane 1) and membrane integration (lane 2) (clones #67 and #68 in reference (Sääf et al., 1998), a kind gift from G. von Heijne's lab). A construct containing the p7B hydrophobic region (amino acids 13–32) was transcribed and translated in vitro in the presence (+) and the absence (−) of MMs (lanes 3 and 4, respectively). Bands of non-glycosylated protein are indicated by a white dot; singly and doubly glycosylated proteins are indicated by one and two black dots, respectively. The H-segment sequence in each construct is shown at the bottom.

ruled out given the presence of a non-glycosylated protein band. The nature of the former protein band (~70%) was confirmed by Endo H treatment (Fig. 3c). The degree of protein glycosylation was quantified from the SDS-PAGE gels by measuring the fraction of glycosylated versus glycosylated plus non-glycosylated bands. To confirm the C-terminal luminal orientation of this chimera, the transcription/translation product was treated with proteinase K. Digestion with proteinase K would degrade the proteins (or a portion of the protein) protruding from the exterior face of the MMs, while proteins (or a portion of the protein) oriented towards the lumen are protected. As shown in Fig. 3d, the proteinase K treatment rendered undigested glycosylated protein bands with a slightly higher electrophoretic mobility, suggesting that only the Nt (10–12 amino acids) would be proteolytically degraded. Interestingly, the non-glycosylated band was almost totally digested, which suggests that a fraction

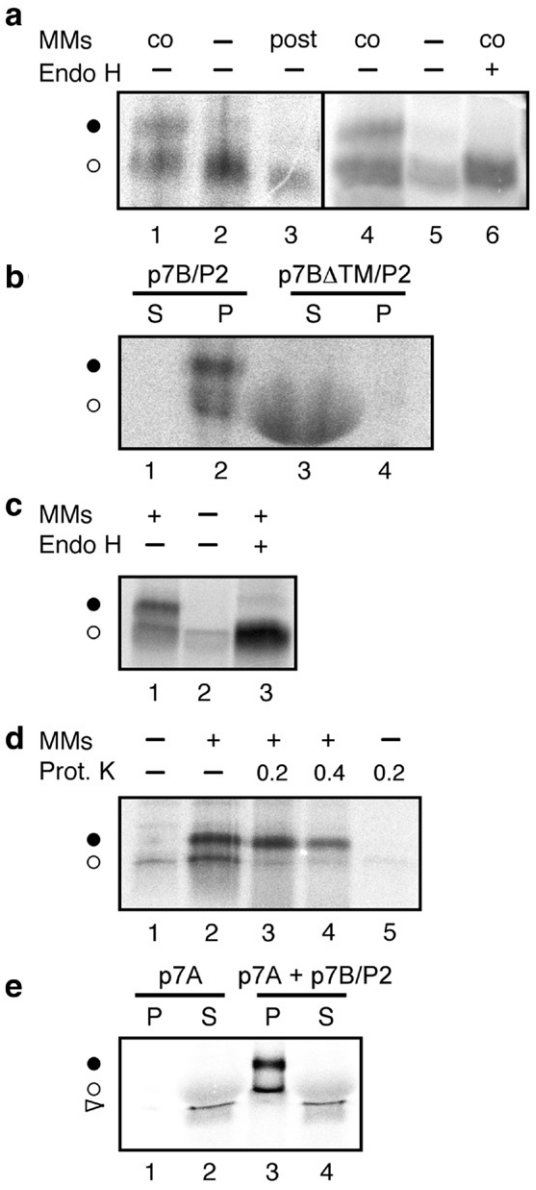

Fig. 3. Co-translational insertion and topology of p7B into the microsomal membrane. (a) p7B was translated in either the absence (lanes 2, 3 and 5) or the presence (lanes 1, 4 and 6) of MMs. In lane 3, MMs were added post-translationally (after 1 h) and incubation was continued for another 1 h. In lane 6, the p7B construct was translated in the presence of MMs and treated later with endoglycosidase H (Endo H), a glycan-removing enzyme. (b) The luminal P2 domain from Lep was fused at the Ct of p7B (p7B/P2). In the p7BΔTM/P2 construct, the p7B TM segment (amino acids 13–32) was deleted. In vitro translated p7B/P2 and p7BΔTM/P2 constructs in the presence of MMs were fractionated into either a soluble fraction (S) or a membrane-enriched fraction (P) by differential centrifugation, as described in Materials and methods. (c) The p7B/P2 construct was translated in vitro in either the presence (+) or the absence (−) of MMs; the identity of the higher molecular weight band was verified by Endo H treatment (lane 3) prior to SDS-PAGE. (d) Proteinase K treatment. p7B/P2 was translated and analyzed for sensitivity mild (0.2 mg/mL, lanes 3 and 5) and harsh (0.4 mg/mL, lane 4) proteinase K treatment in both the presence (lanes 2–4) and the absence of MMs (lanes 1 and 5). (e) p7B/P2 was translated in the presence of p7A. Separately transcribed pGEM–p7B/P2 and pGEM–p7A were co-translated in the presence of MMs. Subsequently, translation mixtures were fractionated into either a soluble fraction (S) or a membrane-enriched fraction (P) by differential centrifugation. The white dots identify the non-glycosylated proteins, the black dots indicate glycosylated polypeptides and the arrowhead identifies p7A.

of protein molecules (<30%) did not properly integrate into the membrane or they were inserted with the reversed topology.

To assess the effect of its partner (p7A) on the observed p7B/P2 topology, in vitro co-translation experiments were performed. Separately in vitro transcribed mRNAs of both sequences were co-translated in vitro in the presence of MMs. After translation termination, samples were subjected to membrane sedimentation in order to verify the presence of both polypeptides in the translation mixtures. As expected, p7A was found in the supernatant fraction with a higher electrophoretic mobility than p7B/P2 (Fig. 3e). As can be seen p7B/P2 is strongly glycosylated (Fig. 3e, lane 3), suggesting that the Ct of the protein is translocated even when p7B/P2 is translated in the presence of p7A.

p7B topology in E. coli membranes

In order to gain topological information in cell membranes we used GFP fusions as a topology reporter in *E. coli* cells. GFP is efficiently folded in a reducing environment (Feilmeier et al., 2000). For this reason, GFP fusions in the cytoplasm are expected to be fluorescent, whereas those in the periplasm are not (Drew et al., 2002). To determine whether GFP fusions would provide reliable results, we used two model C-terminal GFP fusions to the membrane proteins Lep (wild-type sequence which has a periplasmic Ct) and Lep-*inv* (a Lep variant with a cytoplasmic Ct) (kind gifts from G. von Heijne's Lab) (Drew et al., 2002). When tested under the fluorescence microscope, Lep/GFP was indeed found to be non-fluorescent, while Lep-*inv*/GFP was seen to be fluorescent (Fig. 4a), as expected. GFP fusion to the Ct of p7B was created (p7B/GFP), and cells turned to be non-fluorescent under the microscope (Fig. 4a, third panel). Topology inversion can be achieved in membrane proteins, at least partially, by sequence optimization according to the positive-inside rule (von Heijne, 1986), that is, each protein is orientated in such a way that the side containing the higher number of positively charged residues faces the cytoplasm. Since p7B contains one positively charged residue in both extramembrane regions (N- and C-termini, see Fig. 1a), we decided to create a mutant to skew the positive charge distribution in our GFP fusion. The introduction of three lysine residues after residue 32 rendered the fusion p7B3K/GFP. Interestingly, computer-assisted analysis of this modified p7B sequence with several of the above-mentioned programs predicted that this construct should adopt a reversed N-terminal out/C-terminal cytoplasmic topology (data not shown). As ex-

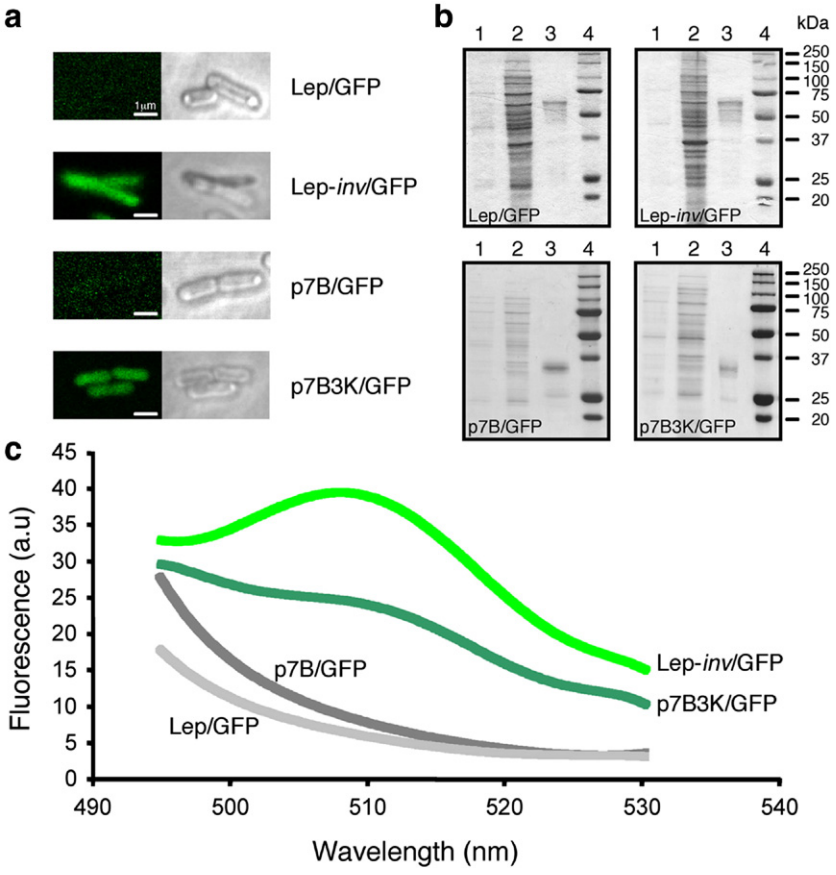

Fig. 4. p7B topology in *E. coli* cell membranes using GFP fusions as a marker. (a) Fluorescence microscope analysis of *E. coli* cells expressing the GFP fused to the Ct of the analyzed proteins. Cells were prepared for analysis as described in Materials and methods. White light exposures of the cells are shown to the right and UV-excited images to the left. Cells containing the fusions Lep/GFP, Lep-inv/GFP, p7B/GFP and p7B3K/GFP are shown. (b) Overexpression and purification of GFP fusion proteins. Coomassie staining of SDS-PAGE gels representing fusion proteins purification by Ni^{2+}-NTA chromatography. Lane 1, uninduced cells; lane 2, induced cells; lane 3, purified fusion proteins; lane 4, molecular weight markers. (c) GFP fluorescence emission spectra of cells expressing the GFP fusion proteins grown at 37 °C.

pected, cells expressing this fusion were seen to be fluorescent under the microscope (Fig. 4a, bottom panel). The fusion proteins were overexpressed, purified using Ni^{2+}–NTA chromatography and analyzed by SDS-PAGE to verify the expression of all constructs (Fig. 4b). The presence of the GFP moiety in all fusions was confirmed by means of immunoblotting with a GFP antibody (not shown). The amount of protein synthesis was used to normalize the activity of the GFP fusion proteins in a fluorometer. Typical GFP fluorescence emission spectra from liquid cultures (whole cells) expressing Lep/GFP, Lep-*inv*/GFP, p7B/GFP and p7B3K/GFP are shown in Fig. 4c. When grown at 37 °C, only those cells expressing the Lep-*inv*/GFP and p7B3K/GFP fusions displayed the typical emission at 508 nm (Fig. 4c), confirming the results observed under the microscope and reinforcing the predominant N-terminal cytoplasmic/C-terminal outside topology of p7B, as preciously observed in the glycosylation experiments.

Membrane insertion and topology of the putative p14 protein

Cell-to-cell movement of carmoviruses is apparently controlled by two small proteins working in trans, an RNA-binding protein (p7A in the MNSV) and a membrane-anchored protein (p7B in the MNSV), referred to as double-gene-block proteins, DGBps (Navarro et al., 2006). The ORFs of the homologous small hydrophobic proteins from TCV and CarMV have overlapping regions. However, MNSV DGBps are exceptional among sequenced carmovirus as both proteins are arranged in frame separated by an amber (TAG) stop codon in such a way that a fusion protein consisting of the complete p7A–p7B ORFs could be synthesized by a read-through process (Riviere and Rochon, 1990) leading to putative p14. Several lines of evidence strongly suggest that p14 is unlikely to play a role in local spread, for example: (i) p14 was unable to promote cell-to-cell movement even in the presence of p7A or p7B (Genoves et al., 2006); (ii) an ochre (TAA) termination codon exists at the end of p7A ORF in some MNSV isolates (Diaz et al., 2003). Of all known 'leaky' stop codons, TAA is by far the least frequently used (Beier and Grimm, 2001). However, the possibility that p14 would participate in the infectious cycle of MNSV in some virus–host combinations cannot be ruled out. Thus, we decided to investigate the membrane insertion capacity and the topology of this putative p14. To this end, we generated the fusion p7A–p7B, referred to as p14, by replacing the amber codon to a tyrosine codon (Fig. 5a). As before, the first 50 residues of the extramembranous P2 domain from Lep were fused in frame at the Ct of p14 to generate p14/P2. In vitro transcription/translation of p14/P2 in either the presence or absence of MMs was analyzed by SDS-PAGE and the glycosylation pattern was followed by autoradiography (Fig. 5b). As above, glycosylation was observed with the appearance of a larger protein in the translation products when translation was conducted in the presence of MMs (compare lanes 1 and 2, Fig. 5b). The nature of this protein was confirmed by a deglycosylation assay (Fig. 5b, lane 3). Alkaline extractions of these samples were performed in order to verify the membrane integration of this p14/P2 chimera (Fig. 5b, lanes 4 and 5). These experiments suggested that in the case of an effective read-through of the amber stop codon located between p7A and p7B, the putative p14 protein would become an integral membrane protein with the N-terminal region (containing the RNA-binding domain (Navarro et al., 2006)) facing the cytoplasm, and with the Ct translocated into the lumen of the ER, that is, with the same topology as p7B.

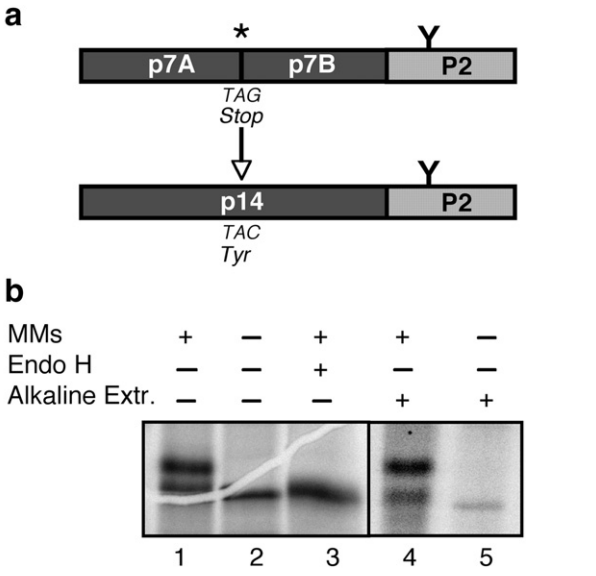

Fig. 5. p14 topology. (a) Schematic representation of the p14/P2 chimera. Fusing p7A and p7B ORFs yielded the p14 expression by replacing the amber stop codon (*TAG*), denoted by an asterisk as in Fig. 1, into a tyrosine (*TAC*) codon mutation at the end of p7A. The first 50 amino acids from the Lep P2 domain were fused in frame at the end of p7B. (b) In vitro translation was performed in both the presence (+) and the absence (−) of MMs and Endo H as indicated. Alkaline extractions of the translation products are shown in lanes 4 and 5. The P2 N-glycosylation site is highlighted by a Y-shaped symbol.

Discussion

This study investigates the topology of the p7B MP of the MNSV. p7B together with its partner p7A have been revealed to be sufficient to support viral movement between adjacent cells operating in trans (Genoves et al., 2006). p7A has been shown to bind RNA and is expected to bind the viral genome in the cell-to-cell transport process, while p7B is involved in the association with the cellular membrane network (Navarro et al., 2006). Even though p7A and p7B form separate subunits, they exhibit a tight functional coupling (Genoves et al., 2006). To better understand how these two movement proteins cooperate it is important to know how p7B is localized in the membrane, this being the objective of the present research. In this study, we have made use of two commonly used strategies to determine membrane protein topology. Firstly, N-glycosylation sites have been used to ascertain membrane integration and the topology of p7B in vitro in the presence of ER-derived membranes. Secondly, we also made use of GFP fusions to verify the glycosylation data in cellular membranes.

Computer-assisted membrane protein topology prediction is a useful starting point for experimental studies of membrane proteins. We have used five popular prediction methods and all

of them agree identifying a single TM domain located in the region between residues 11–16 and 30–34 in the p7B sequence depending on the program used. Moreover, the five algorithms used, predicted an N-terminal cytoplasmic/C-terminal outside orientation for the p7B MP. It should be noted that the reliability of a topology prediction can be estimated by the number of prediction methods that agree (Nilsson et al., 2000); hence the topology prediction for p7B can be ranked as very likely to be correct in bioinformatic terms.

By testing the membrane insertion of the hydrophobic region of p7B in a model protein construct we firstly demonstrated that this region of the viral movement protein fully integrates as TM in the presence of ER-derived membranes. Furthermore, the significant glycosylation of full-length p7B and p7B/P2 fusions, together with the low level of fluorescence of the p7B/GFP construct, demonstrate that MNSV p7B MP preferentially integrates, both in vitro and in *E. coli* membranes, with its Nt facing the cytoplasm and its Ct being translocated across the membrane. Nevertheless, the possibility that p7B could achieve multiple membrane topologies should not be ruled out, as previously seen for other viral membrane proteins (Moise et al., 2004).

Topological studies using biochemical approaches have been performed for other plant virus movement proteins. In a seminal study, p9 MP from CarMV was shown to hold two TM segments and to position both its N- and C-termini towards the cytoplasm. More recently, a model in which the *Tomato ringspot nepovirus* X2 protein traverses the membrane at least three times represents another example of plant viral polytopic membrane protein (Zhang and Sanfacon, 2006). In this context, the small hydrophobic *Beet yellows virus* (BYV) p6 MP was considered unique among other MPs since it is monotopic, that is, it only holds one TM segment (Peremyslov et al., 2004). Similarly, p7B also contains one TM segment, but these last two MPs differ in their membrane orientation as BYV p6 has a cytosolic Ct (Peremyslov et al., 2004), while our results support a C-terminal outside orientation for MNSV p7B. Taken into account the current model for the viral genome transport between adjacent cells in viruses from the genus *Carmovirus*, the MNSV p7B C-terminal translocation across the ER-membrane was somehow unexpected. The interaction between the RNA-bound soluble MP and its membrane-anchored counterpart has been proposed to occur through the Ct of the membrane-anchored protein, at least in the case of CarMV (Vilar et al., 2002). This apparent discrepancy in the C-terminal orientation between p7B and both the BYV p6 and CarMV p9 MPs admits at least four possible explanations according to the differences between these viral systems. First, homologous proteins with opposite C-terminal orientations have been described for both prokaryotic (Daley et al., 2005) and eukaryotic (Kim et al., 2006) membrane proteins. Furthermore, although most membrane proteins are expected to adopt only one topology in the membrane, due to their vectorial function, a dual-topology (i.e. a single polypeptide that inserts into the membrane in two opposite orientations) has been proposed as a plausible evolutionary path for membrane proteins (Rapp et al., 2006, 2007). The second argument assumes that the N-terminal extramembranous domain is larger in p7B than in the other two MPs (BYV p6 and CarMV p9). This enlarged cytoplasmic Nt would allow the membrane-anchored protein to interact with other viral or host components required to accomplish intra- and intercellular steps in cell-to-cell movement. A third possibility would rely on the potential modification of the cellular membranes by p7B being required to promote MNSV movement. In fact during infection, ER membranes aggregate to form inclusions that function as virus factories (Heinlein et al., 1998; Reichel and Beachy, 1998) that contain viral RNA in addition to replicase and MPs (Mas and Beachy, 1999). The replication complex has also been localized more recently on the tonoplast where a reorganization of these membranes induced by virus infection has been suggested (Hagiwara et al., 2003). A fourth possibility is that the presence of p7A would modify the p7B topology in planta. Both p7A and p7B are translated from the same sgRNA. Since p7A ORF precedes the p7B ORF, it is expected that p7A would be synthesized prior to p7B, and that p7A would be more abundant than p7B in MNSV-infected cells, as demonstrated for the equivalent MPs of TCV (Li et al., 1998). Finally, the highly unlikely existence of p14 cannot be excluded. Hence, a few copies of the putative fusion protein p14, synthesized in a read-through process, would be sufficient to anchor a large complex formed by the viral RNA genome and several copies of p7A into the cellular membrane. This functional complementation between p14 and p7A could not be proved using a different complementation approach by individual inoculation onto melon cotyledons (Genoves et al., 2006). However, the fact that most plant membrane proteins are expressed at moderate to low levels, and that the protein expression levels of functional partners should be fine-tuned in viral infections, should be taken into account.

In short, the results from the in vitro and the in *E. coli* whole-cells experiments strongly support a defined membrane topology for the MNSV p7B MP. Further investigations addressing the assessment of the integral membrane protein topology in living plant cells, by means of novel developed techniques like bimolecular fluorescence complementation (Zamyatnin et al., 2006), should lead to a more complete understanding of the role of membranes and MPs in virus infection and cell-to-cell spread. Experiments are currently in progress to know whether the topology observed in MMs and in *E. coli* also operates in planta.

Materials and methods

Computer-assisted analysis of p7B topology

Prediction of transmembrane helices and membrane topology for the p7B sequence was performed using five of the most commonly used topology prediction methods available on the Internet: TMHMM (Krogh et al., 2001) (http://www.cbs.dtu.dk/services/TMHMM/), HMMTOP (Tusnady and Simon, 1998, 2001) (http://www.enzim.hu/hmmtop/), MEMSAT (Jones, 2007; Jones et al., 1994) (http://www.bioinf.cs.ucl.ac.uk/psipred/psiform.html), PHD (Rost et al., 1996) (http://www.cubic.bioc.columbia.edu/pp/) and TOPPRED (Claros and von Heijne, 1994; von Heijne, 1992) (http://www.bioweb.pasteur.fr/

seqanal/interfaces/toppred.html). All user-adjustable parameters were left at their default values.

Enzymes and chemicals

All enzymes as well as plasmid pGEM1, RiboMAX SP6 RNA polymerase system, rabbit reticulocyte lysate and canine pancreatic microsomes were obtained from Promega (Madison, WI). [^{35}S]Met and ^{14}C-methylated markers were attained from GE Healthcare. Restriction enzymes and Endoglycosidase H were from Roche Molecular Biochemicals. The DNA plasmid, RNA clean up and PCR purification kits were from Qiagen (Hilden, Germany). The PCR mutagenesis kit QuikChange was from Stratagen (La Jolla, CA). All the oligonucleotides were from Isogen (Maarseen, The Netherlands).

DNA manipulations

The hydrophobic region from p7B was introduced into the modified Lep sequence from the pGEM1 plasmid (Hessa et al., 2005a) between the *Spe*I and *Kpn*I sites using two double-stranded oligonucleotides with overlapping overhangs at the ends. The complementary oligonucleotides pairs were first annealed at 85 °C for 10 min followed by slow cooling to 30 °C, after which the two annealed double-stranded oligos were mixed, incubated at 65 °C for 5 min, cooled slowly to room temperature and ligated into the vector (a kind gift from G. von Heijne's lab).

The full-length p7B sequence (without a stop codon) fused to the P2 domain of the *E. coli* leader peptidase in a pGEM1 plasmid was described previously (Navarro et al., 2006). By subcloning p7A sequence into *Nco*I/*Nde*I restriction sites in the pGEM-Lep vector (Nilsson and von Heijne, 1993) a plasmid pGEM-p7A was created. Green fluorescent proteins (GFP) fusions were expressed from a vector (a kind gift from J.W. de Gier's lab) constructed by Waldo et al. (Waldo et al., 1999) and modified by Drew et al. (Drew et al., 2001), in which the p7B sequence was cloned between the *Nde*I and *Bam*HI sites by PCR amplification. The substitution of the Asn 49 by Met in the p7B/P2 construct, the insertion of three lysines after residue 32 to generate p7B3K/GFP construct, and the replacement of the amber stop codon (*TAG*) by a tyrosine codon (*TAC*) in the p14/P2 construct were performed using the QuikChange mutagenesis kit from Stratagene (La Jolla, CA) following the manufacturer's protocol.

All DNA manipulations were confirmed by sequencing of plasmid DNAs.

Expression in vitro

Lep constructs with H-segments inserts were transcribed and translated as previously reported (Vilar et al., 2002).

Full-length p7B DNA was amplified from p7B/P2 plasmid using a reverse primer with a stop codon at the end of the p7B sequence (p7B-derived expressions). Alternatively p7B fused to the first 50 amino acids from P2 was amplified using a reverse primer with a stop codon at the 3′ end (p7B/P2-derived expressions). The transcription of the DNA derived from the pGEM1 plasmid was performed as previously described (Vilar et al., 2002). Briefly, the transcription mixture was incubated at 37 °C for 2 h. The mRNAs were purified using a Qiagen RNeasy clean up kit and verified on 1% agarose gel.

In vitro translation of in vitro transcripted mRNA was performed in the presence of reticulocyte lysate, [^{35}S]Met and dog pancreas microsomes as described previously (Garcia-Saez et al., 2004; Vilar et al., 2002). After translation samples were analyzed by SDS-PAGE and gels were visualized on a Fuji FLA3000 phosphorimager using the ImageGauge software.

For endoglicosidase H (Endo H) treatment, the translation mixture was diluted in 4 volumes of 70 mM sodium citrate (pH 5.6) and centrifuged (100 000 × g 20 min 4 °C). The pellet was then suspended in 50 μL of sodium citrate buffer with 0.5% SDS and 1% β-mercaptoethanol, boiled 5 min and incubated 1 h at 37 °C with 0.1 milliunits of Endo H. Then, the samples were analyzed by SDS-PAGE.

For the proteinase K protection assay, the translation mixture was subjected to 100 μg/mL proteinase K digestion for 40 min on ice. The reaction was stopped by adding 2 mM PMSF and was then analyzed by SDS-PAGE.

Co-translational and post-translational insertion assay

Full-length p7B mRNAs were translated (37 °C for 1 h) either in the presence (+ and co samples) or the absence (− and post samples) of microsomal membranes. Translation was then inhibited with cycloheximide (2 mg/mL final concentration) for 10 min at 26 °C and microsomes were added to those samples labelled as post-translational. After an additional hour (37 °C) of incubation membranes were collected by ultra-centrifugation and analyzed by SDS-PAGE.

Membrane sedimentation and alkaline wash

The translation mixture was diluted in 8 volumes of buffer A (35 mM Tris–HCl at pH 7.4 and 140 mM NaCl) for the membrane sedimentation or 4 volumes of buffer A supplemented with 100 mM Na_2CO_3 (pH 11.5) for the alkaline wash. Samples were incubated on ice for 30 min and clarified by centrifugation (10,000×*g* 20 min). Membranes were collected by ultracentrifugation (100,000×*g* 20 min 4 °C) of the supernatant onto 50 μL sucrose cushion. Pellets (P) and supernatants (S) of the ultracentrifugation were analyzed by SDS-PAGE.

Expression of GFP-fusion proteins in E. coli membranes

GFP-fusion plasmids were transformed in *E. coli* Bl21(DE3) pLysS. A single colony was grown overnight at 37 °C in LB medium containing 50 μg/mL kanamycin and 30 μg/mL chloramphenicol. Overnight cultures were diluted 1:50 in 20 mL of fresh medium with antibiotics and grown at 37 °C. When O.D. reached 0.4–0.5 IPTG was added to a final concentration of 0.4 mM, then cells were grown for another 3 h. Then, cells were harvested and resuspended in 1 mL of buffer containing 50 mM Tris–HCl at pH 8.0, 200 mM NaCl and

15 mM EDTA. Following the resuspension, cells were stored at room temperature for 2 h to enhance GFP folding, and were used directly to collect emission spectra between 495 and 530 nm with an excitation at 485 nm in a Perkin Elmer LS 50 fluorometer. For a more detailed protocol see (Drew et al., 2006). In order to visualize whole-cell cultures, 10 μL of the cell suspensions were fixed by adding the same volume of a 4% agarose solution, positioned on a microscopic glass slide and covered with a coverslip. Samples were initially observed under white light, and the same field was then analyzed by using UV laser excitation at 488 nm and recording the emission wavelengths between 500 and 600 nm under a Leica TCS-SP confocal microscope (SCSIE, Universitat de Valèncía). Both white light and UV-excited images were recorded for each field.

Acknowledgments

We thank Cristina Moya and María Gómez for excellent technical assistance, Gunnar von Heijne and Jan-Willem de Gier for generously donating plasmids, and Daniel O. Daley and IngMarie Nilsson for sharing protocols. This work was supported by grants BMC2006-08542 from the Spanish Ministry of Education and Science and ACOMP07/119 from the Generalitat Valenciana (to I.M.). L.M-G. was a recipient of a fellowship from the Universitat de Valencia and M.V. was a postdoctoral fellow from the Juan de la Cierva Programme.

References

Beier, H., Grimm, M., 2001. Misreading of termination codons in eukaryotes by natural nonsense suppressor tRNAs. Nucleic Acids Res. 29 (23), 4767–4782.

Citovsky, V., Zambryski, P., 1991. How do plant virus nucleic acids move through intercellular connections? BioEssays 13 (8), 373–379.

Citovsky, V., Wong, M.L., Shaw, A.L., Prasad, B.V., Zambryski, P., 1992. Visualization and characterization of tobacco mosaic virus movement protein binding to single-stranded nucleic acids. Plant Cell 4 (4), 397–411.

Claros, M.G., von Heijne, G., 1994. TopPred II: an improved software for membrane protein structure prediction. CABIOS 10, 685–686.

Daley, D.O., Rapp, M., Granseth, E., Melen, K., Drew, D., von Heijne, G., 2005. Global topology analysis of the *Escherichia coli* inner membrane proteome. Science 308 (5726), 1321–1323.

Diaz, J.A., Bernal, J.J., Moriones, E., Aranda, M.A., 2003. Nucleotide sequence and infectious transcripts from a full-length cDNA clone of the carmovirus Melon necrotic spot virus. Arch. Virol. 148 (3), 599–607.

Drew, D.E., von Heijne, G., Nordlund, P., de Gier, J.W., 2001. Green fluorescent protein as an indicator to monitor membrane protein overexpression in *Escherichia coli*. FEBS Lett. 507 (2), 220–224.

Drew, D., Sjostrand, D., Nilsson, J., Urbig, T., Chin, C.N., de Gier, J.W., von Heijne, G., 2002. Rapid topology mapping of *Escherichia coli* inner-membrane proteins by prediction and PhoA/GFP fusion analysis. Proc. Natl. Acad. Sci. U. S. A. 99 (5), 2690–2695.

Drew, D., Lerch, M., Kunji, E., Slotboom, D.J., de Gier, J.W., 2006. Optimization of membrane protein overexpression and purification using GFP fusions. Nat. Methods 3 (4), 303–313.

Feilmeier, B.J., Iseminger, G., Schroeder, D., Webber, H., Phillips, G.J., 2000. Green fluorescent protein functions as a reporter for protein localization in *Escherichia coli*. J. Bacteriol. 182 (14), 4068–4076.

Fujiki, M., Kawakami, S., Kim, R.W., Beachy, R.N., 2006. Domains of tobacco mosaic virus movement protein essential for its membrane association. J. Gen. Virol. 87 (Pt 9), 2699–2707.

Garcia-Saez, A.J., Mingarro, I., Perez-Paya, E., Salgado, J., 2004. Membrane-insertion fragments of Bcl-xL, Bax, and Bid. Biochemistry 43 (34), 10930–10943.

Genoves, A., Navarro, J.A., Pallas, V., 2006. Functional analysis of the five melon necrotic spot virus genome-encoded proteins. J. Gen. Virol. 87 (Pt 8), 2371–2380.

Hagiwara, Y., Komoda, K., Yamanaka, T., Tamai, A., Meshi, T., Funada, R., Tsuchiya, T., Naito, S., Ishikawa, M., 2003. Subcellular localization of host and viral proteins associated with tobamovirus RNA replication. EMBO J. 22 (2), 344–353.

Heinlein, M., Epel, B.L., 2004. Macromolecular transport and signaling through plasmodesmata. Int. Rev. Cytol. 235, 93–164.

Heinlein, M., Padgett, H.S., Gens, J.S., Pickard, B.G., Casper, S.J., Epel, B.L., Beachy, R.N., 1998. Changing patterns of localization of the tobacco mosaic virus movement protein and replicase to the endoplasmic reticulum and microtubules during infection. Plant Cell 10 (7), 1107–1120.

Hessa, T., Kim, H., Bihlmaier, K., Lundin, C., Boekel, J., Andersson, H., Nilsson, I., White, S.H., von Heijne, G., 2005a. Recognition of transmembrane helices by the endoplasmic reticulum translocon. Nature 433 (7024), 377–381.

Hessa, T., White, S.H., von Heijne, G., 2005b. Membrane insertion of a potassium-channel voltage sensor. Science 307 (5714), 1427.

Johnson, A.E., van Waes, M.A., 1999. The translocon: a dynamic gateway at the ER membrane. Annu. Rev. Cell Dev. Biol. 15 (2), 799–842.

Jones, D.T., 2007. Improving the accuracy of transmembrane protein topology prediction using evolutionary information. Bioinformatics 23 (5), 538–544.

Jones, D.T., Taylor, W.R., Thornton, J.M., 1994. A model recognition approach to the prediction of all-helical membrane protein structure and topology. Biochemistry 33, 3038–3049.

Kim, H., Melen, K., Osterberg, M., von Heijne, G., 2006. A global topology map of the *Saccharomyces cerevisiae* membrane proteome. Proc. Natl. Acad. Sci. U. S. A. 103 (30), 11142–11147.

Krogh, A., Larsson, B., von Heijne, G., Sonnhammer, E.L., 2001. Predicting transmembrane protein topology with a hidden Markov model: application to complete genomes. J. Mol. Biol. 305 (3), 567–580.

Lazarowitz, S.G., Beachy, R.N., 1999. Viral movement proteins as probes for intracellular and intercellular trafficking in plants. Plant Cell 11 (4), 535–548.

Li, W.Z., Qu, F., Morris, T.J., 1998. Cell-to-cell movement of turnip crinkle virus is controlled by two small open reading frames that function in trans. Virology 244 (2), 405–416.

Lucas, W.J., 2006. Plant viral movement proteins: agents for cell-to-cell trafficking of viral genomes. Virology 344 (1), 169–184.

Marcos, J.F., Vilar, M., Perez-Paya, E., Pallas, V., 1999. In vivo detection, RNA-binding properties and characterization of the RNA-binding domain of the p7 putative movement protein from carnation mottle carmovirus (CarMV). Virology 255 (2), 354–365.

Mas, P., Beachy, R.N., 1999. Replication of tobacco mosaic virus on endoplasmic reticulum and role of the cytoskeleton and virus movement protein in intracellular distribution of viral RNA. J. Cell Biol. 147 (5), 945–958.

Melen, K., Krogh, A., von Heijne, G., 2003. Reliability measures for membrane protein topology prediction algorithms. J. Mol. Biol. 327 (3), 735–744.

Moise, A.R., Grant, J.R., Lippe, R., Gabathuler, R., Jefferies, W.A., 2004. The adenovirus E3-6.7K protein adopts diverse membrane topologies following posttranslational translocation. J. Virol. 78 (1), 454–463.

Navarro, J.A., Genoves, A., Climent, J., Sauri, A., Martinez-Gil, L., Mingarro, I., Pallas, V., 2006. RNA-binding properties and membrane insertion of Melon necrotic spot virus (MNSV) double gene block movement proteins. Virology 356 (1–2), 57–67.

Nilsson, I., von Heijne, G., 1993. Determination of the distance between the oligosaccharyltransferase active site and the endoplasmic reticulum membrane. J. Biol. Chem. 268 (8), 5798–5801.

Nilsson, J., Persson, B., von Heijne, G., 2000. Consensus predictions of membrane protein topology. FEBS Lett. 486 (3), 267–269.

Peremyslov, V.V., Pan, Y.W., Dolja, V.V., 2004. Movement protein of a closterovirus is a type III integral transmembrane protein localized to the endoplasmic reticulum. J. Virol. 78 (7), 3704–3709.

Rapp, M., Granseth, E., Seppala, S., von Heijne, G., 2006. Identification and evolution of dual-topology membrane proteins. Nat. Struct. Mol. Biol. 13 (2), 112–116.

Rapp, M., Seppala, S., Granseth, E., von Heijne, G., 2007. Emulating membrane protein evolution by rational design. Science 315 (5816), 1282–1284.

Reichel, C., Beachy, R.N., 1998. Tobacco mosaic virus infection induces severe morphological changes of the endoplasmic reticulum. Proc. Natl. Acad. Sci. U. S. A. 95 (19), 11169–11174.

Riviere, C.J., Rochon, D.M., 1990. Nucleotide sequence and genomic organization of melon necrotic spot virus. J. Gen. Virol. 71 (Pt 9), 1887–1896.

Rost, B., Fariselli, P., Casadio, R., 1996. Topology prediction for helical transmembrane proteins at 86% accuracy. Protein Sci. 5 (8), 1704–1718.

Russo, M., Burgyan, J., Martelli, G.P., 1994. Molecular biology of tombusviridae. Adv. Virus Res. 44, 381–428.

Sääf, A., Wallin, E., von Heijne, G., 1998. Stop-transfer function of pseudo-random amino acid segments during translocation across prokaryotic and eukaryotic membranes. PG - 821-9 251(0014-2956 VI - 251 IP - 3 DP - 1998 Feb 1), 821–829.

Sauri, A., Saksena, S., Salgado, J., Johnson, A.E., Mingarro, I., 2005. Double-spanning plant viral movement protein integration into the endoplasmic reticulum membrane is signal recognition particle-dependent, translocon-mediated, and concerted. J. Biol. Chem. 280 (27), 25907–25912.

Sauri, A., McCormick, P.J., Johnson, A.E., Mingarro, I., 2007. Sec61alpha and TRAM are sequentially adjacent to a nascent viral membrane protein during its ER integration. J. Mol. Biol. 366 (2), 366–374.

Staehelin, L.A., 1997. The plant ER: a dynamic organelle composed of a large number of discrete functional domains. Plant J. 11 (6), 1151–1165.

Tusnady, G.E., Simon, I., 1998. Principles governing amino acid composition of integral membrane proteins: application to topology prediction. J. Mol. Biol. 283 (2), 489–506.

Tusnady, G.E., Simon, I., 2001. The HMMTOP transmembrane topology prediction server. Bioinformatics 17 (9), 849–850.

Vilar, M., Esteve, V., Pallas, V., Marcos, J.F., Perez-Paya, E., 2001. Structural properties of carnation mottle virus p7 movement protein and its RNA-binding domain. J. Biol. Chem. 276 (21), 18122–18129.

Vilar, M., Sauri, A., Monne, M., Marcos, J.F., von Heijne, G., Perez-Paya, E., Mingarro, I., 2002. Insertion and topology of a plant viral movement protein in the endoplasmic reticulum membrane. J. Biol. Chem. 277 (26), 23447–23452.

Vilar, M., Sauri, A., Marcos, J.F., Mingarro, I., Perez-Paya, E., 2005. Transient structural ordering of the RNA-binding domain of carnation mottle virus p7 movement protein modulates nucleic acid binding. ChemBioChem 6 (8), 1391–1396.

von Heijne, G., 1986. The distribution of positively charged residues in bacterial inner membrane proteins correlates with the trans-membrane topology. EMBO J. 5, 3021–3027.

von Heijne, G., 1992. Membrane protein structure prediction—Hydrophobicity analysis and the positive-Inside rule. J. Mol. Biol. 225 (2), 487–494.

Waldo, G.S., Standish, B.M., Berendzen, J., Terwilliger, T.C., 1999. Rapid protein-folding assay using green fluorescent protein. Nat. Biotechnol. 17 (7), 691–695.

Zamyatnin Jr., A.A., Solovyev, A.G., Bozhkov, P.V., Valkonen, J.P., Morozov, S.Y., Savenkov, E.I., 2006. Assessment of the integral membrane protein topology in living cells. Plant J. 46 (1), 145–154.

Zhang, G., Sanfacon, H., 2006. Characterization of membrane association domains within the Tomato ringspot nepovirus X2 protein, an endoplasmic reticulum-targeted polytopic membrane protein. J. Virol. 80 (21), 10847–10857.